Evidence for the formation of stable CO2 hydrates in zeolite Na-Y: Structural characterization by synchrotron X-ray powder diffraction

Accepted Manuscript

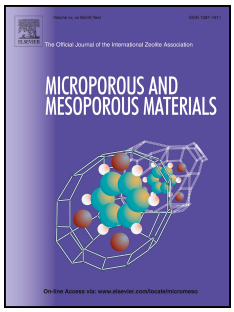

Evidence for the formation of stable CO_2 hydrates in zeolite Na-Y: Structural characterization by synchrotron X-ray powder diffraction

Rossella Arletti, Lara Gigli, Francesco di Renzo, Simona Quartieri

PII: S1387-1811(16)30073-7

DOI: 10.1016/j.micromeso.2016.03.046

Reference: MICMAT 7660

To appear in: *Microporous and Mesoporous Materials*

Received Date: 2 March 2016

Revised Date: 22 March 2016

Accepted Date: 30 March 2016

Please cite this article as: R. Arletti, L. Gigli, F. di Renzo, S. Quartieri, Evidence for the formation of stable CO_2 hydrates in zeolite Na-Y: Structural characterization by synchrotron X-ray powder diffraction, *Microporous and Mesoporous Materials* (2016), doi: 10.1016/j.micromeso.2016.03.046.

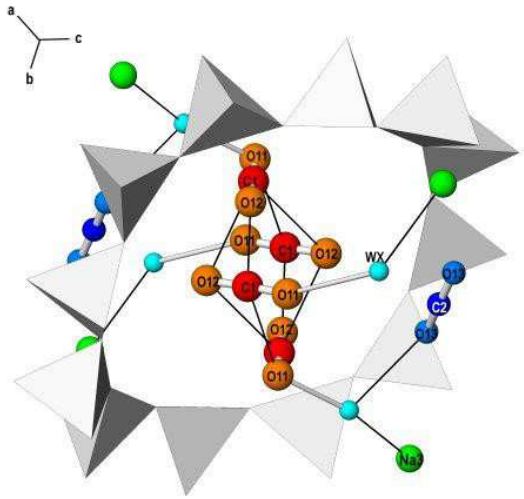

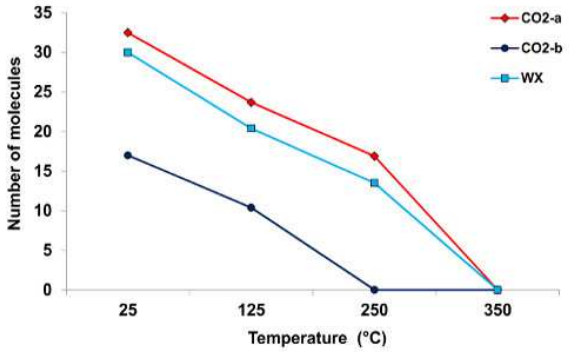

Evidence for the formation of stable CO_2 hydrates in zeolite Na-Y: Structural characterization by synchrotron X-ray powder diffraction

Rossella Arletti[1], Lara Gigli[2], Francesco Di Renzo[3], Simona Quartieri[4]

[1] Dipartimento di Scienze della Terra, Università di Torino, Via Valperga Caluso 35, 10125 Torino, Italy.

[2]Elettra Sincrotrone Trieste, SS14, Km 163.5, 34149 Basovizza TS, Italy

[3] Institut Charles Gerhardt Montpellier, UMR 5253 CNRS-UM-ENSCM, 8 rue Ecole Normale, 34296 Montpellier, France

[4] Dipartimento di Scienze Matematiche e Informatiche, Scienze Fisiche e Scienze della Terra, Università di Messina, Viale Ferdinando Stagno d'Alcontres 31, 98166 Messina S. Agata, Italy

Abstract

Preferential adsorption of water is a major problem in the processes of CO_2 adsorption on molecular sieves. Adsorption and desorption of CO_2 on partially hydrated zeolite Na-Y have been monitored by in situ synchrotron X-ray powder diffraction. The structural refinement of the CO_2-saturated diffraction pattern highlighted the formation of tetrameric CO_2 clusters connected by water bridges to the sodium cations of two adjacent faujasite supercages. The CO_2 desorption was followed by collecting a series of diffraction patterns upon heating from room temperature up to 350°C. The hydrated CO_2 clusters are completely desorbed between 250°C and 350°C. This high thermal stability suggests that the formation of hydrated complexes could represent a potentially important mechanism of retention of CO_2 during the regeneration of CO_2 adsorbents.

Keywords: Na-faujasite; CO_2 adsorption; CO_2 desorption, synchrotron X-ray powder diffraction¸ high temperature structural studies.

1. Introduction

The adsorption of CO_2 by zeolites with faujasite structure (International Zeolite Association structure code FAU [1]) is at the basis of several processes of CO_2 capture and storage. The separation of CO_2 from other light gases on zeolite Na-X (molecular sieve 13X, FAU with Si/Al ratio ~1.25) has been early developed for the purification of natural gas [2], in order to avoid pipeline corrosion by wet acid gases and to comply with the strict purity requirements for cryogenic gas transport. Indeed, zeolite Na-X presents an adsorption capacity and a selectivity higher than most of the other adsorbents for this application [3]. Zeolite adsorbents, and specifically zeolite Na-X, have been also evaluated for the separation of CO_2 from flue gases [4], albeit for the treatment of streams with high CO_2 content at high temperature (HT) the absorption by alkaline solutions remains the industrial standard [5,6].

In all gas separation processes, regeneration of the adsorbent through an efficient desorption of CO_2 by pressure or temperature swing is a critical step in the economics of the processes [7,8]. Thermally stable chemisorption of a fraction of CO_2 can hinder the regeneration of the adsorbent and significantly reduce the sorption capacity in successive adsorption-desorption cycles [9,10]. The most common form of chemisorbed CO_2 is a highly asymmetric carbonate species early observed by Bertsch and Habgood [11]. It was later observed that these carbonate-like species, namely bent CO_2, were only observable on alkaline-exchanged zeolite X and were not formed in the alkaline earth-exchanged form [12,13,14]. This allowed attributing the formation of bent CO_2 to the interaction with cations in site III, exposed at the surface of the supercage and less shielded by lattice oxygen than cations in sites I and II. Indeed, site III is occupied by alkali cations and not by alkaline-earth cations in the dehydrated form of zeolite X [15,16,17].

The formation of more stable mono-dentate carbonates has been observed in the high-temperature treatment of Ca-containing zeolites in the presence of quite low partial pressure of CO_2 [9,18]. The high thermal stability of these carbonate species, which are not decomposed at temperature lower than 700°C, requires special care in the atmosphere control of the high-temperature treatments needed for the shaping of adsorbents or catalysts in a matrix. Stable adsorption of CO_2 impurities can also be a severe drawback in other gas separation processes. Adsorbed CO_2 can compete for the adsorption of other gases and have deleterious effects on the effectiveness of zeolites Li- or Ca-LSX (low silica X, FAU with Si/Al ratio ~1) for the separation of air gases [19].

Competition between the adsorption of CO_2 and water is another phenomenon affecting the CO_2 sorption processes. Preferential adsorption of water was early recognized decreasing by more

than 80 % the CO_2 adsorption capacity of molecular sieve 5A (IZA structure code LTA[1]) from moist atmosphere [20]. In the case of zeolite Na-X, it was shown that the Henry constant of the CO_2 adsorption exponentially decreased with the water loading [21]. As a consequence of competitive water adsorption, the CO_2 capacity of zeolite Na-X decreased by nearly 30 % after a first adsorption cycle from a moist flow [22] and the initial capacity could not be recovered by a thermal treatment at 120 °C [23].

If the detrimental effect of water is well assessed in the usual conditions of the CO_2 sorption processes, a different effect of water was observed at very low pressure. Bertsch and Habgood [11] monitored the adsorption of CO_2 on zeolite X in the presence of pre-adsorbed water. They observed that a small amount of water (2 molecules per unit cell) allowed a faster adsorption of CO_2 on zeolite Na-X. Rege and Yang [24] confirmed that the effect of water on CO_2 adsorption is highly pressure-dependent: the presence of water enhances the adsorption of CO_2 at low relative pressure (less than 200 ppm) and severely decreases the CO_2 uptake at higher pressure.

Most of the previously cited information was the result of experiments based on volumetric adsorption, chromatographic separation and IR spectroscopy of the adsorbed species. These experiments have been more recently complemented by theoretical calculations, which gave useful hints about the position of CO_2 at different loadings. If several studies dealt with the interaction of CO_2 with all-silica zeolites [25,26], some modelling studies provided useful information on the position of CO_2 and its energetics of adsorption in cation-bearing aluminosilicate faujasite adsorbents [27,28,29,30]. While early diffraction studies on FAU allowed locating most of the water molecules of hydrated zeolites (see e.g. [31]) and further diffraction studies have dealt with the location of organic templates and adsorbates in the zeolite cages (see e.g. [32,33,34]), diffraction methods have seldom been applied for locating adsorbed CO_2 [35,36] and, at our knowledge, never for elucidating CO_2-water interactions in zeolite cages.

The interactions between CO_2 and water have been extensively studied outside the zeolite pores, both by experiments and modelling, in the blossoming field of CO_2 hydrates. The field of stability of light gas hydrates has received wide attention as a significant factor in the retention –or liberation– from the oceans of gases with global warming effects. Catastrophic scenarios of autocatalytic global warming have been envisaged, in which ocean warming could destabilize CH_4 and CO_2 sea-bed hydrates, with the release of greenhouse gases [37,38,39]. As CO_2 hydrates are significantly more stable than CH_4 hydrates, it was suggested that, at proper pressure and temperature levels, sea-bed hydrate fields could release recoverable CH_4 and trap injected CO_2, allowing simultaneous exploitation of natural gas reserves and storage of anthropogenic CO_2 [40,41,42].

Several studies have dealt with the stability of CO_2 hydrates segregated in porous materials, in the attempt to simulate sea-bed geological conditions or to propose a hydrate-based technology for CO_2 capture. The stability of CO_2 hydrates inside model silica gels of different pore size has been shown to decrease at the decrease of the pore size from 100 to 6 nm [43,44,45]. However, a stabilisation effect of CO_2 hydrates has been reported in the more confined interlayer space of smectites [46].

In this work we follow the adsorption and desorption of CO_2 molecules in the porosity of a Na-Y zeolite in the presence of water molecules. Through in situ synchrotron X-Ray Powder Diffraction (SR-XRPD) experiments we were able to locate the adsorbed molecules and to describe the CO_2 –CO_2 and CO_2 –H_2O interactions inside the zeolite cavities.

2. Experimental

2.1 Materials

The framework structure of the faujasite (FAU-type framework topology) [1] (Figure 1), is obtained when cuboctahedral sodalite cages (or β-cages) [$4^6 6^8$] are linked together at four of the eight 6-ring windows by double hexagonal rings (D6Rs). The resulting structure is characterized by a tridimensional 12-membered channel system and by large cavities referred to as ‘‘supercages’’ or “α-cages”, with a diameter of approximately 12 Å, interconnected via 12 membered-ring (12MR) windows (7.4 Å free diameter) to four other supercages. The topological symmetry is cubic *Fd*-3*m*, which corresponds to a fully disordered Si/Al distribution.

The zeolite Na-Y of this study was prepared from a synthesis gel made by dissolving 14.17 g NaOH in 160 g deionised water. After cooling back to room temperature (RT), 9.6 g $NaAlO_2$ were added under stirring, followed by 35.4 g Zeosil 175MP precipitated silica. The gel was stirred 24h at RT and heated 14 days at 75°C in a sealed vessel. The solid formed was filtered, washed with deionised water until pH 9 was attained, and dried in air at 80°C. The composition per cell, as determined by elemental and thermogravimetric analyses (for the water content) was $Na_{62}\ Al_{62}\ Si_{130}\ O_{384} \cdot 254\ H_2O$.

2.2. Synchrotron radiation X-ray powder diffraction experiments

2.2.1. XRPD experiment at ambient conditions

A preliminary SR-XRPD experiment at ambient conditions on the Na-Y sample was performed at the SNBL1 (BM01a) beamline at ESRF (Grenoble, France). The diffraction data were collected at λ= 0.69736 Å in the Debye–Scherrer geometry on a Pilatus IP detector (pixel of 172

μm) placed at 193 mm of distance. The powder was placed in a 0.3 mm quartz capillary mounted on a goniometric spinning head. The one-dimensional diffraction pattern was obtained by integrating the two dimensional images with the program FIT2D [47]. Rietveld profile fitting was performed in the *Fd-3* space group (origin at -3) using the GSAS package [48] with the EXPGUI [49] interface, starting from the atomic coordinates reported by Olson [15]. The background curve was fitted using a Chebyshev polynomial with 18 coefficients. The pseudo-Voigt profile function proposed by Thompson et al. [50] was applied and the peak intensity cut-off was set to 0.1% of the peak maximum. The 2θ-zero shift, scale factor, and unit-cell parameters were accurately refined. Soft-restraints were applied to the T–O distances (1.60 Å) and the weight was gradually decreased, after the initial stages of refinement. The isotropic displacement parameters were constrained in the following way: the same value for all tetrahedral cations, a second value for all framework oxygen atoms, and a third value for water oxygen atoms. Details of the structural refinements are reported in Table 1. Atomic coordinates, occupancy factors, and thermal parameters along with bond distances (Å) for Na-Y at RT are reported in Table 2 and Table 3.

2.2.2. XRPD experiment at high temperature and CO_2 adsorption/desorption

The in situ time-resolved SR-XRPD experiments were performed at the MCX beamline of Elettra Sincrotrone Trieste (Italy). The powdered sample of Na-Y was carefully packed inside a 0.5 mm quartz capillary open at both ends. Before the CO_2 adsorption, the sample was degassed in vacuum at 350°C. After degassing, the sample was saturated with CO_2 at 1 bar for 30 minutes. XRPD patterns were collected on an image plate at a fixed wavelength of 0.7498 Å. In the CO_2 sorption process, moisture was admitted and allowed to study the effect of complex sorption. In order to study the CO_2 desorption behavior, a series of patterns were collected upon heating from RT to 350°C with a heating rate of 5°C /min. These conditions ensure the sample dehydration [51].

The wavelength was calibrated using Si as external standard, while temperature calibration was achieved by measuring the thermal expansion of platinum [52] collected under the same experimental conditions. During the heating process, the diffraction patterns were collected every 25 °C on a translating image plate detector and then integrated into one-dimensional powder patterns with the FIT2D software [47]. The structural refinements were carried out with the same strategy used for RT experiments.

Atomic coordinates, occupancy factors, and thermal parameters along with bond distances (Å) for dehydrated Na -Y, CO_2 saturated and CO_2 desorbed sample are reported in Tables 2 and 3.

3. Results and discussion

3.1 Structure of hydrated and dehydrated Na-Y.

The structure of as-synthesized Na-Y is consistent with the model of Olson [15]. 35 Na cations were located (see Figures 1 and 2): 3 in Na1 site (center of the D6R, site I in classical nomenclature [53, 31], 14 in Na2 site (center of six membered ring between sodalite cage and D6R, site I') and 18 in Na3 site (six membered ring face of sodalite cage on the supercage side, site II). The remaining 27 Na cations were not located, being distributed over disordered positions, as typically observed in hydrated synthetic faujasites [15]. 244 water molecules were located over six independent crystallographic sites (namely W2, W4, W6, W8, W9 and W10 in Table 3 and [15]), in very good agreement with thermogravimetric results, indicating the presence of 254 molecules. The Na1 cation – sited in the D6R – is bonded only to framework oxygen atoms, while Na2 and Na3 – sited in the sodalitic cage and in the supercage, respectively – coordinate oxygen atoms of both framework and water molecules in W2. All the other water molecules form clusters in the supercage and have no or weak interactions with the framework (Table 3).

Upon heating of Na-Y, all the water molecules are progressively lost: 201 and 166 water molecules were located at 125°C and 250°C, respectively, whereas at 350°C the zeolite is completely dehydrated. The refinement at 350°C allows locating 62 Na atoms (3 in Na1, 27 in Na2 and 32 in Na3 sites), exactly corresponding to the charge compensation of the 62 Al atoms substituting for Si in the framework. The customary ordering of the cations is induced by the water loss.

3.2 Location of CO_2 and water in saturated Na-Y

The structure of the Na-Y sample after CO_2 adsorption is reported in Figures 2 and 3 and in Tables 2 and 3. 64 Na atoms are located by the refinement (6 in Na1, 26 in Na2 and 32 in Na3 sites), in satisfactory agreement with the chemical analysis. Upon saturation, 49 CO_2 molecules are found in the supercage, distributed over 2 different sites – namely CO_2a and CO_2b – hosting 32 and 17 molecules, respectively. Moreover, as a consequence of moisture admission in the sample after the HT treatment, 30 water molecules were detected in the site WX, bonded to the Na3 cation. This site has no close relation with any of the water sites of the fully hydrated zeolite.

Being any FAU cell formed by 8 supercages, six CO_2 molecules (four CO_2a and two CO_2b, respectively, in red and blue in Figures 2 and 3) are located in any supercage. The experimental sorption isotherms on zeolite Na-Y indicated a loading of about 8 CO_2 molecules per supercage at the equilibrium, with a CO_2 pressure of 1 bar [54,55]. Albeit the presence of unobserved disordered CO_2 cannot be excluded, the presence of water has been reported decreasing the CO_2 capacity [21]

and the observed difference can also be justified by the presence of nearly four molecules of water per supercage in our experiment.

The refined occupancy factors (Table 2) indicate that both CO_2 sites, as well as the WX water site, occupy about 1/3 of the symmetrically equivalent positions. Careful consideration of "impossible" distances between sites and of the steric hindrance of the extraframework species allows establishing a coherent description of the most probable location of the molecules. Concerning the WX site, only four positions (of the twelve sited in each supercage and related by symmetry) do not imply a steric superposition with oxygen atoms of a CO_2 molecule and/or unrealistic bond distances. These WX sites correspond to water molecules bridging Na3 cation and an oxygen atom (O11) of a CO_2a molecule (Figure 3). Moreover, also O13 is at coordination distance. The choice of the CO_2a molecules connected to the WX site is based on mutual superposition avoidance and implies that only four of the twelve symmetrically equivalent positions in the supercage can coexist.

In Figure 3, the resulting arrangement of the CO_2 and water molecules is shown in detail. The main feature is a cluster of four CO_2a molecules (red in figure), equivalent by symmetry, organized in two intertwined slipped parallel pairs rotated of about 60°. The O11 oxygens of the four CO_2a molecules are hydrogen-bonded to four WX water molecules, which are themselves bonded to Na3 cations. The water molecules form bridges between the tetrameric CO_2 cluster and Na3 cations in two different supercages. This confers a peculiar spread-eagled shape to the CO_2a tetramer, which lies across the 12-member ring between the supercages. WX water molecules are statistically hydrogen-bonded to both CO_2a and CO_2b molecules. The CO_2b molecules lie in front of the 4-member ring ladders on the side of the supercage and their C2 atom is very weakly connected to O12 atom of the CO_2a molecule (bond distance 3.69 Å).

If our structural data are compared with the spectroscopic and theoretical ones about CO_2 adsorption on dehydrated faujasites [27], it can be remarked that, in the presence of water, no CO_2 molecules are directly bonded to the Na cations. CO_2 molecules only establish water-mediated interactions with the Na3 cation at the rim of the supercage. The conformation of the hydrated cluster is consistent with the relative affinities of CO_2 and water with the sodium cations. The stronger affinity of water for the sodium cations of the zeolite is well known. The heat of adsorption of water on Na-Y is higher than 60 $kJmol^{-1}$ [56,57] while the heat of adsorption of CO_2 on the same zeolite has been measured between 28 and 36 $kJmol^{-1}$ [58,27]. Clearly, the water molecules more strongly interact with the only cation present in the supercage and prevent the direct coordination of CO_2 molecules with Na3.

The presence of water has also significant implications on the conformation of the CO_2 molecules. Bent CO_2 molecules, corresponding to the formation of carbonate-like species, have often been observed as a result of electron donation from an external oxygen atom [59]. Direct interaction of CO_2 with the cations has been shown to be necessary for the activation of the chemisorption of CO_2 in a bent configuration in the zeolites [60,61]. In our water-CO_2 mixed adsorption system, both bond lengths and O-C-O angles (177° for CO_{2a} and 173° for CO_{2b}) were consistent with essentially linear CO_2 configurations. The saturation of cations by adsorbed water accounts for the absence of bent chemisorbed CO_2.

Spectroscopic data available in the literature seem to indicate that the linear conformation of adsorbed CO_2 is a general effect of water co-adsorption in significant amount. This effect has not been observed at extremely low amounts of adsorbed water. Electron donation by water has indeed been shown to favour the formation of adsorbed bent CO_2 but this effect has been observed when the amount of adsorbed water was low enough (2 molecules per cell [11]) to leave most cations accessible to CO_2. At higher water content, Rege et al. [24] observed that the increase of adsorbed water in Na-X (from 40 to 135 molecules per cell) drastically influenced the ratio between the IR bands at 2360 and 1359 cm^{-1}, corresponding to linear and bent CO_2 species, respectively. Also Galley and Stumpf [18] observed that co-adsorption of water drastically decreased the formation of mono-dentate carbonate species upon CO_2 adsorption, clearly indicating that accessible dehydrated cations are needed for the formation of bent CO_2 species.

The polar environment of the CO_2 cluster in Na-Y is clearly different from the non-polar environment of CO_2 or CH_4 clathrates, the most intensely studied hydrated gas clusters. In the case of the CO_2 clathrates, a continuous network of hydrogen bonds between water molecules forms cages in which isolated CO_2 molecule are trapped in a non-polar environment.[62,63,64]

The conformation of the tetrameric CO_2 cluster in Na-Y is clearly related to its strong coordination with water molecules. The 2.30 Å distance between the O_{11} atom of the CO_2a molecule and the WX water (Table 3) is significantly shorter than a typical hydrogen bond but it is in the range calculated for low-temperature hydrogen-bonded CO_2-water clusters [65]. These four strong bonds draw the molecules of the cluster towards the water-bridged Na3 cations and shift in opposite direction the CO_2a molecules of each parallel pair.

The tetrameric cluster presents a high compactness. The shortest inter-cluster distances between adjacent molecules (3.02 Å C1-C1 and 2.28 Å C1-O12) are significantly shorter than the corresponding 3.97 Å C-C and 3.1 Å C-O distances in dry ice CO_2-I structure.

3.3 CO_2 desorption

After CO_2 saturation, the sample was heated up to 350° C and three diffraction patterns – at 125°C, 250°C and 350°C – were collected with the aim of following the desorption process.

All CO_2 and water molecules adsorbed during the saturation process are released before the highest investigated temperature (Figure 4). Specifically, the molecules in CO_2b site are completely released at 250°C, so appearing the less strongly bonded ones. The strongest bonded CO_2 molecules are those in site CO_2a (completely released only at 350°C). Indeed, the distance between the Na-bonded water WX and CO_2a molecules (WX-O11 = 2.30 Å in Table 3) is significantly shorter than the distance between WX and CO_{2b} molecules (WX-O12 = 2.80 Å in Table 3), confirming a stronger bond between the bridging water and the tetrameric CO_2.

It can be remarked that water molecules in WX site and CO_2 molecules in CO_{2a} are released with the same trend up to the highest investigated temperature. Very likely, this trend corresponds to a non-equilibrium desorption mechanism, in which clusters in different parts of the crystal are destabilized by the decrease of water vapor pressure inside the porosity.

Finally, during heating, the Na3 cation moves away from the interior of the supercage, in parallel with the water molecule desorption (Table 2 and 3).

4. Conclusions

Advanced diffractometric techniques are effective tools to identify the spatial distribution of molecules adsorbed in molecular sieves. The precise location of CO_2 molecules adsorbed in zeolites has been somewhat neglected, albeit being the object of some theoretical studies. In the specific case of co-adsorption of water and CO_2 on molecular sieves, the abundant spectroscopic and calorimetric data up to now available have not been integrated by corresponding detailed descriptions of specific CO_2 siting.

In this work, synchrotron X-ray powder diffraction experiments have allowed defining the location of CO_2 molecules adsorbed on moist Na-Y and has evidenced the formation of an original tetrameric cluster of CO_2 molecules connected to the sodium cations by water bridges. The absence of bent CO_2 in a system in which water coordinate the alkali cations is in good agreement with the spectroscopic evidences pointing to the requirement of a direct CO_2-cations interaction for the formation of carbonate species. The high compactness of the cluster can be attributed to the confined environment of the 12-member window connecting two faujasite supercages.

The high thermal stability of the hydrated CO_2 cluster in Na-Y suggests that the formation of hydrated complexes could represent a potentially important mechanism of retention of CO_2 during the regeneration of CO_2 adsorbents. Further research is needed to understand at which level the formation of complex clusters is a more general phenomenon in co-adsorption on molecular sieves. The development of this field of investigation is strongly supported by the technological implications of the desorption mechanisms in the separation processes.

Acknowledgments

This work was supported by the Italian MIUR, in the frame of the following projects: PRIN2010-11 'Dalle materie prime del sistema Terra alle applicazioni tecnologiche: studi cristallochimici e strutturali' (local scientific responsible SQ) and FIRB, Futuro in Ricerca 'Impose Pressure and Change Technology' (RBFR12CLQD), (local scientific responsible RA). The authors are grateful to Andrea Lausi, Mahmoud Ahmed Abdellatief and Jasper Plaisier for support during the HT-XRPD experiments and to Marie-France Driole for support in the preparation of the materials.

References

[1]Ch. Baerlocher, L.B. McCusker, D.H. Olson, Atlas of Zeolite Framework Types, 6th ed., Elsevier, Amsterdam, 2007
[2] T.E. Rufford, S. Smart, G.C.Y. Watson, B.F. Graham, J. Boxall, J.C. Diniz da Costa, E.F. May, J. Petroleum Sci. Eng. 94-95 (2012) 123-154.
[3] Y.S. Bae, R.Q. Snurr, Angew. Chem. Int. Ed. 50 (2011) 11586-11596.
[4] S. Cavenati, C.A. Grande, A.E. Rodrigues, J. Chem. Eng. Data 49 (2004) 1095-1101.
[5] D. Aaron, C. Tsouris, Sep. Purif. Rev. 40 (2005) 321-348.
[6] Q. Wang, J. Luo, Z. Zhong, A. Borgna, Energy Environ. Sci. 4 (2011) 42.
[7] S. Sircar, Separ. Sci. Technol. 23 (1988) 519-529.
[8] H. Audus, Energy 22 (1997) 217-221.
[9] C.L. Angell, M.V.Howell, Can. J. Chem. Eng. 47 (1969) 3831-3836.
[10] D. Bonenfant, M. Kharoune, P. Niquette, M. Mimeault, R. Hausler, Sci. Technol. Adv. Mater. 9 (2008) 013007.
[11] L. Bertsch, H.W. Habgood, J. Phys. Chem. 67 (1963) 1621–1628.
[12] J.W. Ward, H.W. Habgood, J. Phys. Chem. 70 (1966) 1178-1182.
[13] G. Martra, S. Coluccia, P. Davit, E. Gianotti, L. Marchese, H. Tsuji, H. Hattori, Res. Chem. Intermed. 25 (1999) 77-93.
[14] G. Martra, R. Ocule, L. Marchese, G. Centi, S. Coluccia, Catal. Today 73 (2002) 83-93.
[15] D.H Olson, J. Phys Chem, 74 (1970) 2758-2764.
[16] J.J. Pluth, J.V. Smith, Mater. Res. Bull. 7 (1972) 1311-1322.
[17] T. Frising, P. Leflaive, Micropor. Mesopor. Mat. 114 (2008) 27-63.
[18] E. Galley, G. Stumpf, J. Colloid Interface Sci. 55 (1976) 415-420.
[19] C. Lutz, P.G. Schmitt, WO2005061100.

[20] L. Dell'Osso, J. Winnick, Ind. Eng. Chem. 8 (1969) 469-476.
[21] F. Brandani, D.M. Ruthven, Ind. Eng. Chem. Res. 43 (2004) 8339-8344.
[22] R. Siriwardane, M. Shen, E. Fisher, J. Poston, A. Shamsi, Journal of Energy and Environmental Research (U. S. Department of Energy) 1 (2001) 19-34.
[23] R.V. Siriwardane, M.S. Shen, E.P. Fisher, Energy Fuel. 19 (2005) 1153-1159.
[24] S.U. Rege, R.T. Yang, Chem. Eng. Sci. 56 (2001) 3781-3796.
[25] R. Krishna, J.M. van Baten, Chem.Eng. J. 133 (2007) 121-131.
[26] M. Fischer, R.G. Bell, J. Phys. Chem. C 116 (2012) 26449-26463.
[27] G. Maurin, P.L.Llewellyn, R.G. Bell, J. Phys. Chem. B 109 (2005) 16084-16091.
[28] D.F. Plant, G. Maurin, I. Deroche, L. Gaberova, P.L. Llewellyn, Chem. Phys. Lett. 426 (2006) 387-392.
[29] L. Grajciar, J. Cejka, A. Zukal, C. Otero Arean, G. Turnes Palomino, P. Nachtigall, ChemSusChem 5 (2012) 2011-2022.
[30] L.C. Lin, A.H. Berger, R.L. Martin, J. Kim, J.A. Swisher, K. Jariwala, C.H. Rycroft, A.S. Bhown, M,W. Deem, M. Haranczyk, B. Smit, Nat. Mater. 11 (2012) 633-641.
[31] T. Frising, P. Leflaive, Micropor. Mesopor. Mat. 114 (2008) 27-63.
[32] H. van Koningsveld, H. van Bekkum, J.C. Jansen, Acta Crystallogr. B43 (1987) 127-132.
[33] S. Nair, M.Tsapatsis, J. Phys. Chem. B 104 (2000) 8982-8988.
[34] A. Martucci, A. Alberti, M.L. Guzman-Castillo, F. Di Renzo, F. Fajula, Micropor. Mesopor. Mat. 63 (2003) 33-42.
[35] T.H. Bae, M.R.Hudson, J.A. Mason, W.L. Queen, J.J. Dutton, K.Sumida, K.J. Micklash, S.S. Kaye, C.M.Brown, J.R.Long, Energy Environ. Sci. 6 (2013) 128.
[36] M.R. Hudson, W.L. Queen, J.A. Mason, D.W. Field, R.F. Lobo, C.M. Brown, J. Am. Chem. Soc. 134 (2012) 1970-1973.
[37] J.P.Severinghaus, M.J. Whiticar, E.J. Brook, V.V. Petrenko, D.F. Ferretti, Science 313 (2006) 1109–1112.
[38] M. Kennedy, D. Mrofka, C. Van Der Borch, Nature 453 (2008) 642–645.
[39]J.P. Kennett, K.G. Cannariato, I.L. Hendy, R.J. Behl. Methane Hydrates in Quaternary Climate Change: The Clathrate Gun Hypothesis. Wiley, New York 2003.
[40] K. Ohgaki, K. Takano, H. Sangawa, T. Matsubara, S. Nakano, J. Chem. Eng. Jpn. 29 (1996) 478-483.
[41] P.G. Brewer, G. Friederich, E.T. Peltzer, F.M. Orr, Science 284 (1999) 943-945.
[42] R. Martos-Villa, M. Francisco-Marquez, M.P. Mata, C.I. Sainz-Diaz, J. Mol. Graph. Model. 44 (2013) 253-265.
[43] Y. Seo, H. Lee, T. Uchida, Langmuir 18 (2002) 9164-9170.
[44] X.S. Li, Y. Zhang, G. Li, Z.Y. Chen, K.F. Yan, Q.P. Li, J. Chem. Thermodyn. 40 (2008) 1464-1474.
[45] S.P. Kang, J.W. Lee, H.J. Ryu, Fluid Phase Equilibr. 274 (2008) -72.
[46] R. Martos-Villa, M.P. Mata, C.I. Sainz-Diaz, J. Mol. Graph. Model. 49 (2014) 80-90.
[47] A.P. Hammersley, S.O. Svensson, M. Hanfland, A.N. Fitch, D. Häusermann. High Pressure Res. 14 (1996) 235–248..
[48] A.C. Larson, R.B. Von Dreele. General Structure Analysis System ″GSAS″; Los Alamos National Laboratory Report; Los Alamos,1994; LAUR 86-748.
[49] B.H.J. Toby, EXPGUI, a Graphical User Interface for GSAS. Appl. Crystallogr. 34 (2001) 210−213
[50] P. Thompson, D.E. Cox, J.B. Hastings, J. Appl. Crystallogr. 20 (1987**)** 79–83.
[51] A. Abdoulayea, J.V. Zanchettab, F. Di Renzo, J.C. Giuntinib, J. Vanderschueren, G. Chabanisb Micropor. Mesopor. Mat. 34, (2000) 317–325
[52] P. Riello, A. Lausi, J. Macleod, J. Rikkert Plaisier, G. Zerauschek, P. Fornasiero, J. Synchrot. Rad.. 20 (2013) 194–196.

[53] W.J.Mortier, Compilation of extraframework sites in zeolites, Butterworth 1982.
[54] V.R. Choudhary, S. Mayadevi, A. Pal Singh, J. Chem. Soc. Faraday Trans. 91 (1995) 2935-2944.
[55] K.S. Walton, M.B. Abney, M. D. LeVan, Micropor. Mesopor. Mat. 91 (2006) 78-84.
[56] B. Boddenberg, G.U. Rakhmatkariev, S. Hufnagel, Z. Salimov, Phys. Chem. Chem. Phys. 4 (2002) 4172-4180.
[57] J.P.Bellat, C. Paulin, M.Jeffroy, A. Boutin, J.L.Paillaud, J.Patarin, A. Di Lella, A. Fuchs, J.Phys. Chem. C 113 (2009) 8287-8295.
[58] P.J.E. Harlick, F.H. Tezel, Micropor. Mesopor. Mat. 76 (2004) 71-79.
[59] H.J. Freund, M.W. Roberts, Surf. Sci. Rep. 25 (1996) 225-273.
[60] P.A. Jacobs, F.H. van Cauwelaert, E.F. Vansant, J.B. Uytterhoeven, J. Chem. Soc. Faraday Trans. 69 (1973) 1056-1068.
[61] P.A. Jacobs, F.H. van Cauwelaert, E.F. Vansant, J. Chem. Soc. Faraday Trans. 69 (1973) 2130-2139.
[62] J.A. Ripmeester, C.I. Ratcliffe, Energy Fuels 12 (1998) 197-200
[63] E. D. Sloan, Nature 426 (2003) 353-359.
[64] A.K. Sum, C.A. Koh, E.D. Sloan, Ind. Eng. Chem. Res. 48 (2009) 7457-7465
[65] C.N. Ramachandran, E. Ruckenstein, Comp. Theor. Chem. 966 (2011) 84-90.

Table and Figure captions

Table 1. Details of the X-ray powder diffraction structural refinements.

Table 2. Atomic coordinates, occupancy factors, and isotropic thermal parameters of Na-Y at RT, dehydrated at 350°C, CO_2 saturated at 25°C and after CO_2 desorption at 350°C. Fd-3 origin is at -3.

Table 3. Selected bond distances (Å) for of Na-Y at RT, dehydrated at 350°C, CO_2 saturated at 25°C and after CO_2 desorption at 350°C.

Figure 1. FAU framework projected along [111].

Figure 2. Structure of Na-Y along [110] upon CO_2 adsorption, evidencing the hydrated CO_2 cluster in-between two supercages. Upon saturation, six CO_2 molecules (four CO_2a and two CO_2b respectively, in red and blue) are found in any supercage. As a consequence of moisture admission, 30 water molecules were detected in the site WX, bonded to the Na3 cation.

Figure 3. Location in the 12-membered window of the tetrameric cluster of CO_2a molecules (red) connected by four bridging H_2O molecules (turquoise) to sodium cations (green).

Figure 4. Occupancy variation of CO_2 and water molecules during the high temperature desorption treatment. All CO_2 and water molecules adsorbed during the saturation process are released before the highest investigated temperature. The strongest bonded CO_2 molecules are those in site CO_2a.

Table 1

NaY				
	RT	**Dehydrated (at 350°)**	**CO_2 Saturated (at 25°C)**	**After CO_2 desorption (at 350°)**
Space Group	F d-3	F d-3	F d-3	F d-3
a (Å)	24.7631(2)	24.7846(7)	24.7305(8)	24.747(1)
V (Å3)	15185.0(4)	15224(1)	15125(1)	15155(1)
Rp (%)	4,4	5,14	6,4	8,5
R wp (%)	6,5	6,54	8,3	10,7
R F2 (%)**	9,2	8,5	7,7	7,9
No. of variables	97	68	92	67

Table 2

Atom	x/a	y/b	z/c	Occ.	Uiso
	RT				
T1	-0.0520 (3)	0.1245 (3)	0.0357 (4)	1	0.002(2)
T2	-0.0539(3)	0.0353(4)	0.1266(4)	1	0.002(2)
O1	-0.1108(5)	-0.0022(8)	0.1050(6)	1	0.007(3)
O2	-0.0060(6)	-0.0018(6)	0.1445(3)	1	0.007(3)
O3	-0.0300(3)	0.0761(7)	0.0706(6)	1	0.007(3)
O4	-0.0686(3)	0.0724(7)	0.1775(7)	1	0.007(3)
Na1	0	0	0	0.179(3)	0.018(1)
Na2	0.0656(5)	0.0656(5)	0.0656(5)	0.432(2)	0.013(1)
Na3	0.2407(4)	0.2407(4)	0.2407(4)	0.573(5)	0.046(1)
W2	0.0830(4)	0.0811(7)	0.1777(5)	0.297(4)	0.023(5)
W4	0.3112 (7)	0.2868 (4)	0.2702(7)	0.204(3)	0.058(5)
W6	0.2854(5)	0.2606 (7)	0.3741(5)	0.708(2)	0.102(4)
W8	0.2035(4)	0.3938(5)	0.3040(7)	0.227(3)	0.0764(5)
W9	0.3707(1)	0.3968(5)	0.2128(6)	0.450(4)	0.052(5)
W10	0.2692(1)	0.4310(4)	0.2141(1)	0.666(4)	0.056(3)
	Dehydrated (at 350°)				
T1	-0.0532 (3)	0.1238 (3)	0.0348(4)	1	0.013(1)
T2	-0.0556(3)	0.0376(4)	0.1258(4)	1	0.013(1)
O1	-0.1082(5)	0.0024(8)	0.1064(6)	1	0.023(1)
O2	-0.0006(6)	-0.0023(6)	0.1432(3)	1	0.023(1)
O3	-0.0338(3)	0.0775(7)	0.0766(6)	1	0.023(1)
O4	-0.0685(3)	0.0732(7)	0.1848(7)	1	0.023(1)
Na1	0	0	0	0.210(3)	0.017(1)
Na2	0.0540(5)	0.0540(5)	0.0540(5)	0.825(2)	0.082(1)
Na3	0.2339(7)	0.2339(4)	0.2339(4)	1	0.032(1)
	CO_2 saturated (at 25°C)				
T1	-0.0530(5)	0.1231(4)	0.0349(5)	1	0.005(2)
T2	-0.0532(5)	0.0372(5)	0.1265(5)	1	0.005(2)
O1	-0.1074(5)	0.0027(7)	0.1067(6)	1	0.013(3)
O2	-0.0038(4)	-0.0022(5)	0.1440(4)	1	0.013(3)
O3	-0.0333(4)	0.0742(5)	0.0743(5)	1	0.013(3)
O4	-0.0687(4)	0.0740(5)	0.1827(5)	1	0.013(3)
Na1	0	0	0	0.394(3)	0.018(1)
Na2	0.0587(4)	0.0587(4)	0.0587(4)	0.825(2)	0.013(1)
Na3	0.2374(4)	0.2374(4)	0.2374(4)	1	0.046(1)
C1	0.211(3)	-0.021(3)	-0.328(3)	0.339(1)	0.13(4)
O11	0.168(3)	0.001(3)	-0.332(3)	0.339(1)	0.12(3)
O12	0.254(2)	-0.043(2)	-0.327(2)	0.339(1)	0.09(4)
C2	0.125	-0.042(3)	-0.375	0.353(1)	0.11(3)
O13	0.099(3)	-0.045(3)	-0.333(3)	0.353(1)	0.08(2)
WX	0.041(2)	0.012(2)	-0.335(2)	0.313(1)	0.10(5)

	After CO_2 desorption (at 350°)				
T1	-0.0527(6)	0.1219(6)	0.0350(7)	1	0.009(2)
T2	-0.0564(6)	0.0366(7)	0.1270(6)	1	0.009(2)
O1	-0.1087(8)	0.0046(11)	0.1059(8)	1	0.013(3)
O2	-0.0024(7)	-0.0003(8)	0.1411(6)	1	0.013(3)
O3	-0.0337(6)	0.0756(7)	0.0765(8)	1	0.013(3)
O4	-0.0702(6)	0.0736(7)	0.1857(7)	1	0.013(3)
Na1	0	0	0	0.143(3)	0.024(1)
Na2	0.0509(4)	0.0509(4)	0.0509(4)	0.711(2)	0.082(1)
Na3	0.2327(3)	0.2327(3)	0.2327(3)	0.830(2)	0.047(1)

Table 3

		RT	Dehydrated (at 350°)	CO_2 Saturated (at 25°C)	After CO_2 desorption (at 350°)
Na1	O3 [x6]	2.683(2)	2.830(6)	2.723(2)	2.789(2)
Na2	O2 [x3]	3.115 (2)	2.946(6)	3.017(4)	2.888(2)
	O3 [x3]	2.382(2)	2.323(7)	2.340(4)	2.270(2)
	W2 [x3]	2.863(3)			
	W2 [x3]	2.625(3)			
	W2 [x3]	2.569(3)	-		
Na 3	O2 [x3]	2.433(2)	2.330(7)	2.375(2)	2.358(15)
	O4 [x3]	2.944(2)	2.808(7)	2.860(3)	2.825(16)
	W2 [x3]	3.026(2)			
	WX			2.81(1)	
W2 -	O2	3.118(3)			
	O2	2.880(2)			
	O2	2.918(2)			
	Na2	2.863(3)			
	Na2	2.569(3)			
	Na2	2.625(3)			
	Na3	3.026(2)			
	W2 [x3]	3.170(3)			
	W2	3.005(3)			
W4 -	W6	2.729(2)			
	W6	2.526(2)			
	W8	2.664(2)			
	W9	2.750(2)			
W6 -	W4	2.729(2)			
	W4	2.526(2)			
	W9	3.001(3)			
	W10	2.267(2)			
	W10	2.996(2)			
W8 -	O1	2.869(2)			
	W4	2.664(3)			
	W9	2.378(2)			
	W10	2.906(2)			
	W10	2.199(2)			
	W10	2.576(2)			
W9 -	W4	2.750(2)			
	W6	3.001(3)			
	W6	2.057(2)			
	W8	2.378(2)			
	W10	2.653(3)			
W10 -	W6	2.267(2)			
	W6	2.996(3)			
	W8	2.906(2)			
	W8	2.199(2)			
	W8	2.576(2)			
	W9	2.653(3)			
	W10[x2]	3.180(2)			
	W10[x2]	2.370(2)			

WX -	Na3			2.81(2)	
	O11			2.30(9)	
	O11			3.17(8)	
	O13			2.80(1)	
C1	O11			1.2003(4)	
	O11			2.721(9)	
	O11			3.36(1)	
	O12			1.2003(4)	
	O12			3.050(1)	
	O12			2.277(3)	
O11	C1			1.2003(4)	
	C1			2.721(9)	
	C1			3.36(1)	
	WX			3.17(1)	
	WX			2.30(1)	
O12	C1			1.2003(4)	
	C1			2.277(3)	
	C1			3.050(1)	
	C2			3.69(2)	
C2	O13[X2]			1.2003(3)	
	O12			3.69(2)	
O13	C2			1.200(3)	
	WX			2.80(1)	

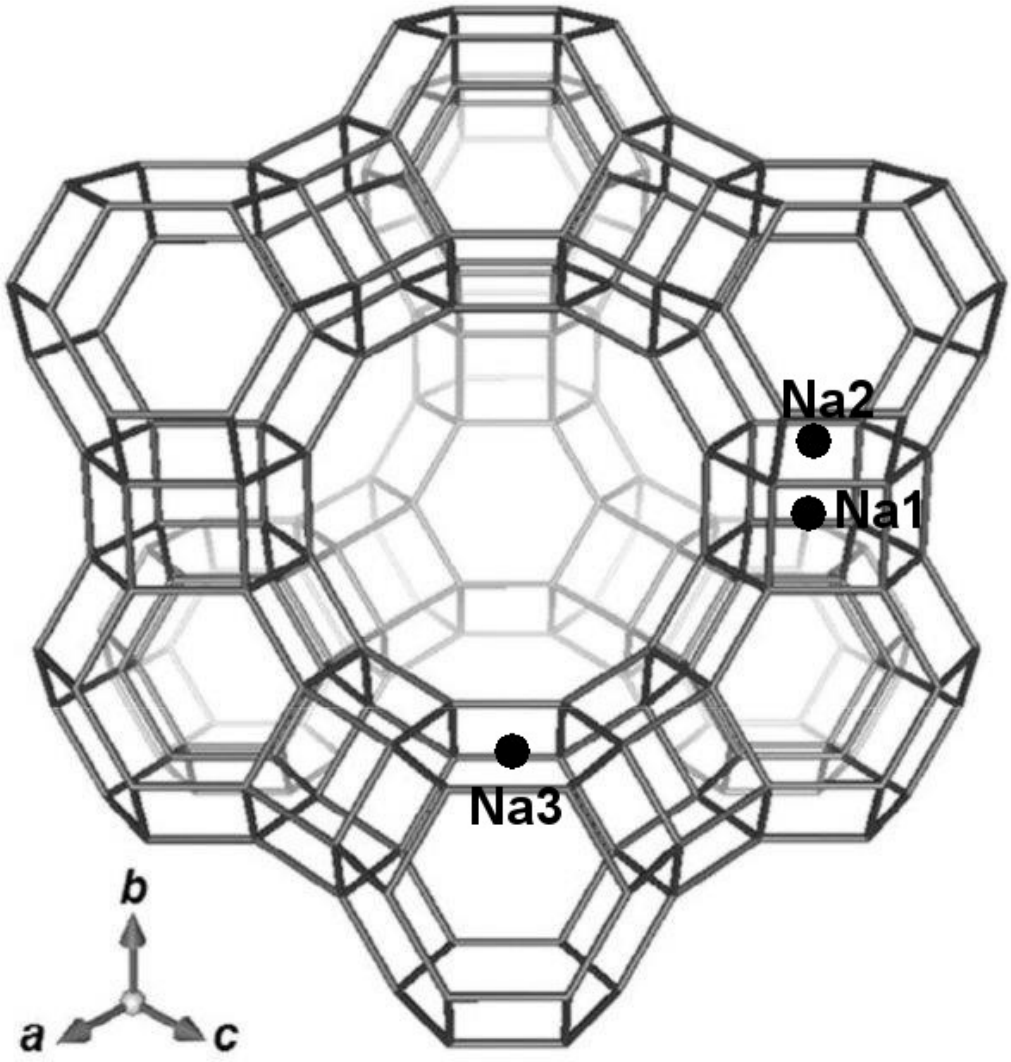

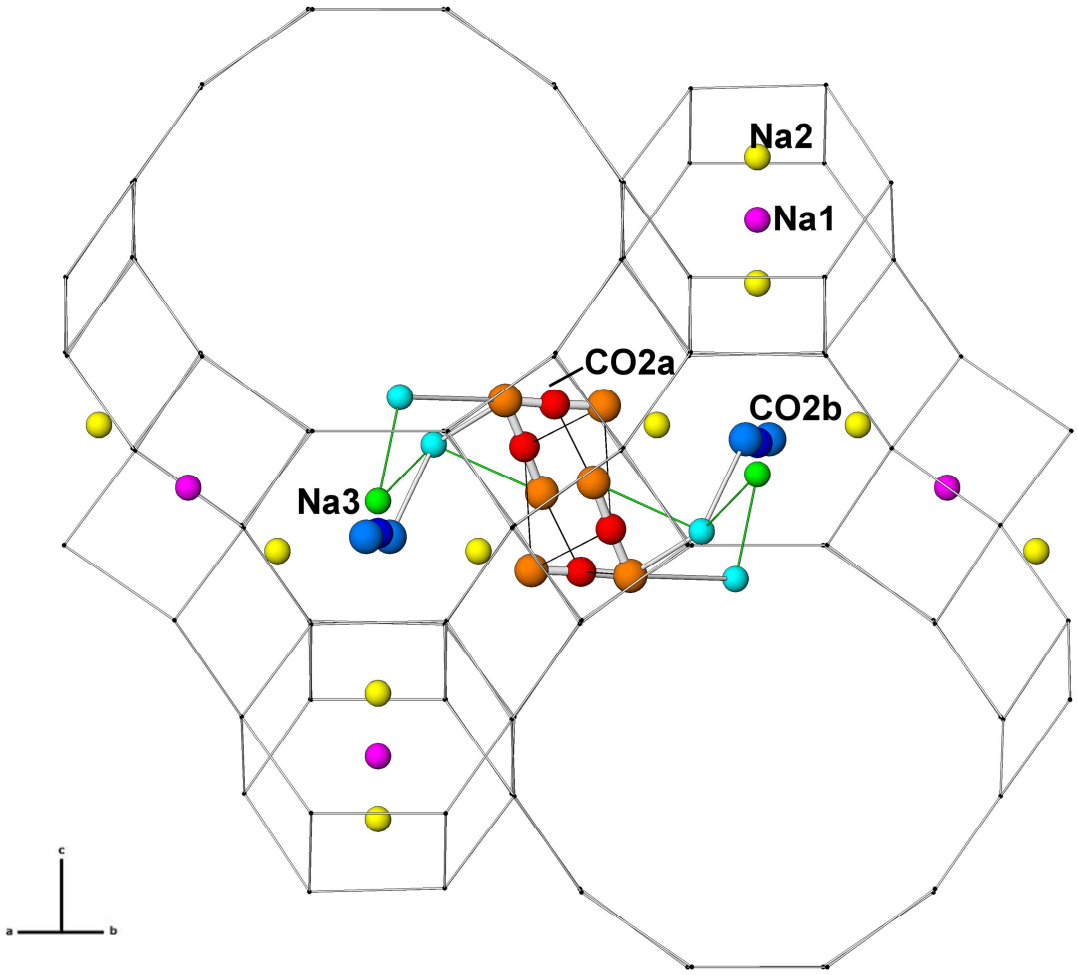

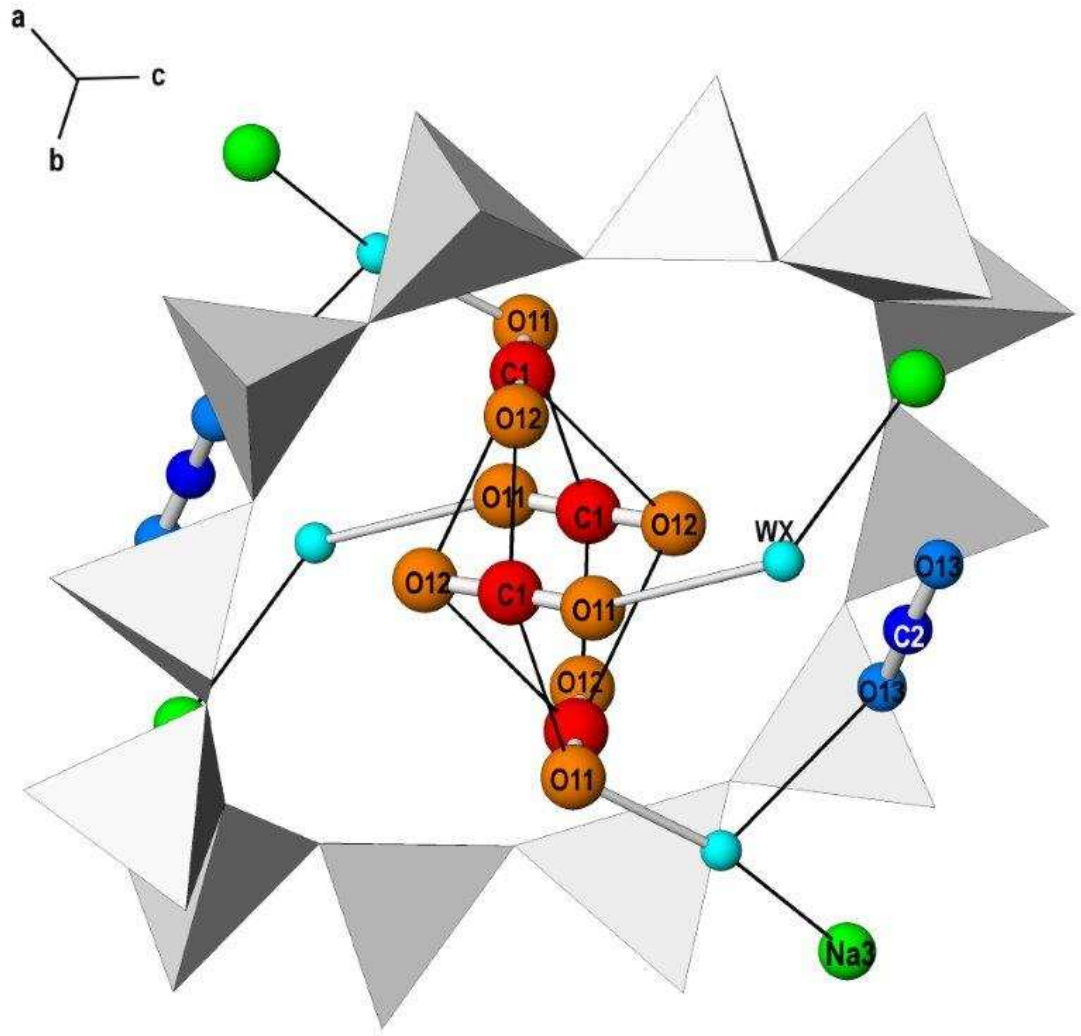

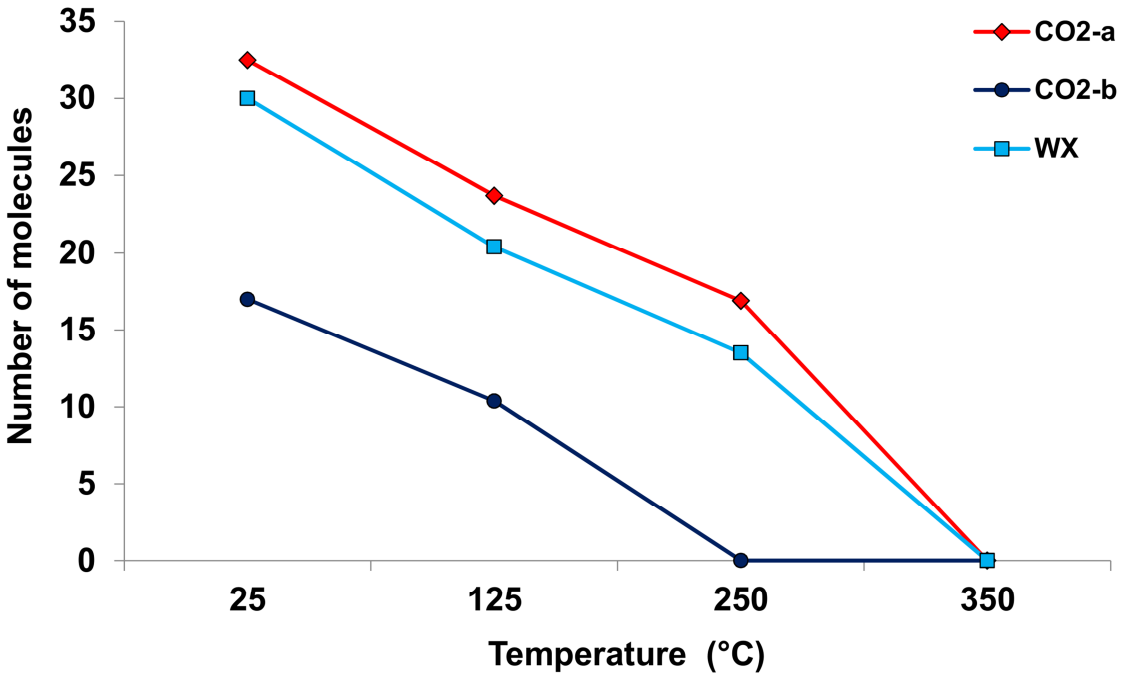

Evidence for the formation of stable CO_2 hydrates in zeolite Na-Y: structural characterization by Synchrotron Radiation - X-Ray Powder Diffraction

HIGHLIGHTS

- Adsorption/desorption of CO_2 have been monitored on partially hydrated zeolite Na-Y.
- Tetrameric clusters of CO_2 molecules are confined between two FAU supercages
- CO_2 clusters are connected to the sodium cations by water bridges
- The hydrated CO_2 clusters are completely desorbed between 250 and 350°C